JLB JOURNAL OF LEUKOCYTE BIOLOGY

HIGHLIGHTED ARTICLE

The cation channel TRPM8 influences the differentiation and function of human monocytes

Eve Hornsby[1] | Hamish W. King[1] | Madusha Peiris[2] | Roberto Buccafusca[3] | Wing-Yiu Jason Lee[1] | Elinor S. Wing[1] | L. Ashley Blackshaw[2] | James O. Lindsay[1,4] | Andrew J. Stagg[1]

[1]Centre for Immunobiology & Barts and The London School of Medicine & Dentistry, Queen Mary University of London, London, UK

[2]Centre for Neuroscience & Trauma, Blizard Institute, Barts and The London School of Medicine & Dentistry, Queen Mary University of London, London, UK

[3]School of Biological and Chemical Sciences, Queen Mary University of London, Mile End Road, London, UK

[4]Department of Gastroenterology, Barts Health NHS Trust, The Royal London Hospital, Whitechapel, London, UK

Correspondence
Andrew J. Stagg, Centre for Immunobiology & Barts and The London School of Medicine & Dentistry, Queen Mary University of London, London E1 2AT, UK.
Email: a.stagg@qmul.ac.uk

Additional supporting information may be found in the online version of the article at the publisher's website.

Abstract

Monocytes are mononuclear phagocytes that can differentiate to a variety of cell fates under the influence of their microenvironment and hardwired commitment. We found that inhibition of TRPM8 in human blood $CD14^+$ monocytes during a critical 3-h window at the beginning of their differentiation into macrophages led to enhanced survival and LPS-driven $TNF\alpha$ production after 24 h. TRPM8 antagonism also promoted LPS-driven $TNF\alpha$ production in $CD14^+$ monocytes derived from the intestinal mucosa. Macrophages that had been derived for 6 days under blockade of TRPM8 had impaired phagocytic capacity and were transcriptionally distinct. Most of the affected genes were altered in a way that opposed normal monocyte to macrophage differentiation indicating that TRPM8 activity promotes aspects of this differentiation programme. Thus, we reveal a novel role for TRPM8 in regulating human $CD14^+$ monocyte fate and function.

KEYWORDS
LPS, monocyte-derived macrophage, phagocytosis, TRP channels

1 | INTRODUCTION

are mononuclear phagocytes, which, in adult life, develop from bone marrow (BM) progenitors and migrate to peripheral tissues via the bloodstream. They function as integral components of the immune response to pathogens and contribute to tissue repair,[1,2] but are also involved in the pathogenesis of conditions such as atherosclerosis, inflammatory disease, and cancer.[3–7] Classical monocytes

$(CD14^+CD16^-)$ make up 80–90% of human blood monocytes and represent the most newly formed subset.[8] They circulate for approximately 1 day before either differentiating further within the blood into nonclassical $(CD14^{low}CD16^+)$ monocytes via an intermediate $(CD14^+CD16^+)$ stage or undergoing extravasation to enter lymph nodes and tissues.[9–11] Within tissues, monocytes can maintain their monocyte-like state and act as effector cells in their own right or differentiate to give rise to functionally diverse monocyte-derived populations including macrophages and dendritic cells.[9,12–14] The regulation of these diverse developmental trajectories is poorly understood but considered to be influenced at a tissue level by microenvironmental cues such as cytokines,[15,16] microbial and dietary compounds,[9,17,18] and notch signaling.[19] Monocyte cell fate and function is also to some degree preprogrammed during myelopoesis.[20]

Abbreviations: AMTB, *N*-(3-Aminopropyl)−2-[(3-methylphenyl) methoxy]-*N*-(2-thienylmethyl) benzamide hydrochloride; BM, bone marrow; DiSBAC₂3, Bis-(1,3-diethylthiobarbituric acid) trimethine oxonol; GO, gene ontology; LPMC, lamina propria mononuclear cell; M8-Ag, 4-[5-(4-chlorophenyl)−4-phenyl-4H-1,2,4-triazol-3-yl]morpholine; M8-B, *N*-(2-Aminoethyl)-*N*-[[3-methoxy-4-(phenylmethoxy)phenyl]methyl]−2-thiophenecarboxamide hydrochloride; MFI, mean fluorescence intensity; Mo-M, monocyte-derived macrophage; SBP, specific blocking peptide; TRP, transient receptor potential; TRPM8, transient receptor potential melastatin 8.

The transient receptor potential (TRP) channels are a family of ligand-gated cation channels that are widely expressed throughout mammalian tissues. They act as cellular sensors, responding to stimuli such as temperature, voltage, mechanical stimulation, lipids, proteins, and metabolites.[21] Ligand-induced activation of these channels leads to a cation influx that contributes to changes in membrane voltage and influences cellular processes.

TRP channels expressed by immune cells play critical roles in their function.[22] Notably, the activity of TRPA1 and TRPV1 regulates TCR-induced Ca^{2+} influx to control T cell inflammatory properties[23,24]; TRPM7 influences the development and early activation of B cells[25,26] as well as LPS-induced activation in macrophages[27]; and TRPM2 dampens ROS production[28] and is critical for inflammasome activation in macrophages.[29]

TRPM8 is well characterized as a cold receptor in sensory neurons[30,31] although was originally cloned from human prostate tissue.[32] In addition to its activation by cold temperatures (<28°C) and cooling compounds such as menthol, icilin, and eucalyptus,[30,31] factors that influence TRPM8 channel activity include phosphatidylinositol 4,5-bisphosphate $(PI(4,5)P_2)$,[33] G proteins,[34] lysophospholipids,[35,36] testosterone,[37,38] and the thyroid hormone derivative, 3-iodothyronamine.[39] TRPM8 has diverse extraneuronal expression where it regulates cellular functions such as proliferation, motility, cytokine production, and thermogenesis.[40–43] A role for TRPM8 in immune cell function has been emerging since the first report of TRPM8-like channels in the macrophage RAW-264.7 cell line using electrophysiologic patch clamp analysis.[44] Since then, expression of TRPM8 has been demonstrated in murine peritoneal macrophages[45] and murine T cells.[46] Mice deficient for TRPM8 are hypersusceptible to experimentally induced colitis[22,47] and treatment with a TRPM8 agonist reduces the severity of this disease,[45,48] indicating that TRPM8 activation has a protective role in intestinal inflammation. In keeping with this observation, TRPM8 RNA levels are elevated in the mucosa of Crohn's disease patients and in colonic tissue of mice with experimentally induced colitis.[48] Importantly, there is evidence that the association of TRPM8 with intestinal inflammation is the result of altered TRPM8 activity in macrophages. The adoptive transfer of TRPM8-deficient macrophages leads to exacerbation of colitis[45] and in vitro activation of TRPM8 in murine peritoneal macrophages promotes an anti-inflammatory, highly phagocytic profile.[45]

The precise contribution of TRPM8 channel activity to the differentiation and function of cells in the human monocyte/macrophage lineage remains completely unknown. Consistent with the murine data, we found that TRPM8 is expressed in cells of the monocyte/macrophage lineage in humans. We have shown that pharmacologic inhibition of TRPM8 influences membrane potential in human monocytes and has time-dependent downstream effects on monocyte survival, inflammatory capacity, and their differentiation into macrophages. We therefore establish for the first time an essential role for TRPM8 in the regulation of human monocyte/macrophage differentiation and function.

2 | MATERIALS AND METHODS

2.1 | Tissues and cells

Peripheral blood samples were derived from healthy volunteers who had given written informed consent (ethical approval: 05/Q0405/71). PBMCs were obtained by centrifugation in Ficoll®Paque PLUS (GE Healthcare) and CD14$^+$ monocytes were isolated by positive selection using CD14 MicroBeads (Miltenyi Biotec). Colonic biopsies were collected from individuals undergoing investigation for altered bowel habit who were consented under ethical approval (15/LO/2127). The colonic tissue was treated with 1 mM DTT (Sigma–Aldrich) to remove feces and mucus followed by 1 mM EDTA (Sigma–Aldrich) in HBSS to remove the epithelial layer. The remaining tissue was digested with 1 mg/ml collagenase D (Sigma–Aldrich) in RPMI 1640 medium (HEPES modification; Sigma–Aldrich) containing 2% FBS and 20 μg/ml DNase 1 (Sigma–Aldrich). The resultant lamina propria mononuclear cell (LPMC) preparation was passed through a 40 μm strainer before culture. The prostate carcinoma cell line DU145 (ATCC) was propagated in complete growth medium (DMEM containing 10% FBS, 100 U/ml penicillin, and 100 μg/ml streptomycin) as per the recommended protocol. For immunohistochemistry, resection tissue from inflammatory bowel disease patients undergoing surgical removal of diseased tissue at the Royal London Hospital was obtained under full written consent (East London and The City HA Local Research Ethics Committee [NREC 09/H0704/2]).

2.2 | Immunohistochemistry

Tissue was fixed in 4% paraformaldehyde overnight at 4°C. Tissues were cryoprotected in 30% sucrose/PBS then mounted in optimum cutting temperature medium. Tissue sections of 10 μm were cut on a Cryostat (Leica CM1860), incubated with blocking buffer (Dako, UK) for 1 h, and primary antibodies were applied overnight (4°C): TRPM8 (1:200; Alomone Labs; ACC-049), CD64 (1:500; Dako; C727801-2). Tissues were washed (PBS; 3 × 5 min) and species-specific secondary antibodies conjugated to Alexa Fluor fluorescent dyes (1:400; Thermo Fisher Scientific, UK) applied for 1 h, before washing (PBS; 3 × 5 min), mounting (Vectashield® hard set mounting media; Vector Laboratories, USA) and cover-slipping. Immunoreactivity of sections was visualized on a Leica DM4000 epi-fluorescence microscope and images were captured using MetaMorph software (Molecular Devices, UK).

2.3 | Antibody labeling for flow cytometry

Cell viability in blood monocyte and LPMC cultures was determined using fixable viability dye (BioLegend) according to the manufacturers' protocol. Staining for monocyte surface markers was performed in FACS buffer (Ca^{2+} and Mg^{2+}-free PBS containing 2% FBS, 0.02% NaN_3 and 1 mM EDTA) for 30 min on ice with anti-human CD14 FITC

(Clone HCD14; BioLegend), anti-human CD45 PE (Clone HI30; BioLegend), and anti-human HLA-DR (Clone L243; BioLegend) antibodies. Staining for intracellular TNFα was achieved by fixation and permeabilization of the cells using Leucoperm™ reagents (Bio-Rad) and staining with anti-human TNFα PE or PE CY7 (Clone Mab11; BioLegend) on ice for 30 min. Counting beads were added in some experiments to determine cell number.

For the detection of TRPM8 protein by flow cytometry, freshly isolated CD14$^+$ monocytes, monocyte-derived macrophages (Mo-M) or DU145 cells were fixed using Leucoperm™ fixative. Cells were then preincubated for 15 min at room temperature with Leucoperm™ permeabilization reagent plus human TruStainFcX™ (Biolegend) to block nonspecific binding. TRPM8 staining was achieved by further incubation of the cells on ice for 1 h after the addition of anti-TRPM8 antibody (Clone ACC-049; Alomone) alone at a final concentration of 8 μg/ml, or in combination with 8 μg/ml of specific blocking peptide. Secondary antibody staining was performed on ice for 30 min using donkey anti-rabbit (abcam; final concentration 1 μg/ml). All samples were acquired on a FACSCanto II (BD Biosciences) and analyzed using Flowjo® version 8 and 10.

2.4 | Cell culture

Peripheral blood CD14$^+$ monocytes were differentiated into Mo-M by culturing 0.5×10^6 cells per ml in complete RPMI 1640 medium (Dutch modification containing 10% FBS, 100 U/ml penicillin, 100 μg/ml streptomycin, and 2 mM L-glutamine) in the presence of M-CSF (100 ng/ml; PeproTech) for 6 days at 37°C. In some experiments, cells were analyzed after 3 or 24 h of this differentiation culture. Where indicated, icilin (10 μM; Tocris Bioscience), N-(3-Aminopropyl)−2-[(3-methylphenyl) methoxy]-N-(2-thienylmethyl) benzamide hydrochloride (AMTB) hydrate (10 μM; Sigma–Aldrich), 4-[5-(4-chlorophenyl)−4-phenyl-4H-1,2,4-triazol-3-yl]morpholine (M8-Ag) (10 μM; gift from Takeda Pharmaceuticals San Diego), N-(2-Aminoethyl)-N-[[3-methoxy-4-(phenylmethoxy)phenyl]methyl]−2-thiophenecarboxamide hydrochloride (M8-B) (10 μM; Tocris Bioscience), PMA (100 ng/ml), or DMSO (Sigma–Aldrich) were also added at the beginning of the differentiation culture. Fresh complete medium containing M-CSF and additional drugs was supplied at day 3.

LPMCs were cultured at 1×10^6 cells per ml in complete RPMI 1640 medium in the presence of AMTB hydrate (10 μM; Sigma–Aldrich) or DMSO (Sigma–Aldrich) for 24 h.

To determine the TNFα response to LPS, CD14$^+$ blood monocytes or LPMCs that had been cultured for 24 h were exposed for a further 3 h in 100 ng/ml LPS from Escherichia coli O111:B4 (Sigma–Aldrich) or not, in the presence of 3 μM monensin (Sigma–Aldrich), after which time intracellular staining for TNFα was performed as described above.

2.5 | Quantitative PCR analysis

Total RNA was isolated from freshly isolated CD14$^+$ monocytes, Mo-M or DU145 cells using an RNAeasy Mini kit PLUS (Qiagen) according to the manufacturers' protocol. RNA quantification was performed using a nanodrop and cDNA was synthesized using a high-capacity cDNA reverse transcription kit (Applied Biosystems; ThermoFisher Scientific). Quantitative real time PCR was performed using QuantiFast SYBR green mix (Qiagen) and Quantitect PCR primers (GAPDH: QT00079247, TRPM8: QT00038906). Samples were run on a 7500 real-time cycler (Applied Biosystems; ThermoFisher Scientific)

2.6 | Determination of membrane potential

Bis-(1,3-diethylthiobarbituric acid) trimethine oxonol (DiSBAC$_2$(3)) (Invitrogen™; ThermoFisher Scientific) was added to the culture medium at a final concentration of 1 μM and was incubated at 37°C for 30 min. Cells were then harvested and washed out of the dye before acquisition on a FACSCanto II (BD Biosciences). Data were analyzed using Flowjo® version 8.

2.7 | RNA sequencing and data analysis

Total RNA was isolated from freshly isolated CD14$^+$ monocytes or Mo-M differentiated in the presence of either DMSO or AMTB using an RNAeasy Mini kit PLUS (Qiagen) according to the manufacturers' protocol. RNA libraries ($n = 5$) were prepared for massively parallel sequencing using the NEBNext Ultra II Directional RNA Library Prep Kit (NEBL). Libraries were assessed using the Agilent TapeStation and quantified using Qubit HS DNA kit prior to sequencing on the NextSeq 500 with 75 bp paired end reads. Transcript counts were generated using Salmon[49] against the GRCh38 transcriptome (Ensembl release 92). Tximport[50] was used to collapse multiple transcripts per gene into a single expression estimate for each protein-coding gene. Differential expression analysis was performed using DESeq2 with default settings.[51] Nonexpressed genes were defined as having a mean log$_2$ expression level < 5 and were removed. All analysis was carried out using R Studio version 3.4.4. Gene ontology (GO) analysis was performed using Metascape.[52] The datasets generated are available under GEO accession number: GSE131415.

2.8 | Phagocytosis and endocytosis assays

CD14$^+$ monocytes or Mo-M differentiated in the presence of DMSO or AMTB were prepared at 1×10^6 cells per ml in complete RPMI. Fluoresbrite® YG Carboxylate Microspheres (Polyscience; 2 μm) or FITC-dextran (Sigma; 4 kDa) were added at a concentration of 1×10^7 particles/ml or 1 mg/ml, respectively and then incubated at 37°C for 1.5 h. Control (4°C) samples were chilled on ice for 1 h prior to the addition of the microspheres or FITC-dextran (4 kDa) and then incubated on ice for an equivalent period of time. Ice cold PBS was added to stop the reactions. Samples were washed and acquired on a FACSCanto II (BD Biosciences). Data were analyzed using Flowjo® version 8.

2.9 | Cellular membrane protein enrichment

About 30 million CD14$^+$ monocytes were collected and sonicated in cold PBS supplemented with protease inhibitors. Following centrifugation at 13,000 × g for 10 min, the insoluble fraction containing cellular membranes was separated from the supernatant and delipidated following a modified Bligh and Dyer lipid extraction procedure.[53,54] Briefly, 1 ml of chloroform (Sigma–Aldrich) was added and the mixture was shaken for 1 h at room temperature. One milliliter of MeOH:H$_2$0 (1:1) was then added and the organic and the polar phases were partitioned following vigorous mixing of the sample and centrifugation at 2000 × g for 1 min. The interphase containing the hydrophobic membrane proteins was isolated, washed twice with cold acetone, and then dissolved in 50 μl of 8 M urea (Sigma–Aldrich) prepared in 50 mM ammonium bicarbonate pH 8.0. Total protein content was determined using a bicinchoninic acid assay (Pierce™ BCA Protein Assay Kit).

2.10 | In-solution digestion of membrane proteins

Fifty micrograms of total protein was digested with Trypsin Gold (Promega, UK) in the presence of 8 M urea in 50 mM ammonium bicarbonate pH 8.0 and the surfactant ProteaseMaxTM (Promega). The sample was reduced in 5 mM DTT at 37°C for 1 h, and alkylated in 15 mM iodoacetamide at ambient temperature for 20 min. Trypsin digestion was performed at an enzyme-to-protein ratio of 1:25 at 37°C for 16 h. Peptides were collected by centrifugation and acidified with formic acid to a concentration of 0.5%.

2.11 | Liquid chromatography-high resolution mass spectrometry/electrospray ionization

Liquid chromatography-high resolution mass spectrometry (LC-HRMS)/electrospray ionization analysis was carried out using an Acquity H Class UPLC system (Waters, Manchester, UK) coupled to a Waters Synapt G2-Si mass spectrometer. Mobile phase A contained 0.1% formic acid in water, and mobile phase B contained 0.1% formic acid in acetonitrile. Peptide samples corresponding to approximately 1000 ng of digested protein were separated on an analytical column (BEH300 C18 100 mm × 2.1 mm, 1.7 μm column; Waters) at a flow rate of 200 μl/min using a gradient from 5% to 43% B over 38 min. Information on precursor and fragment ions was acquired by executing scan at low and elevated collision energy.

2.12 | HRMS data processing and protein identification

UNIFI 1.9 (Waters) was used for raw data processing and to compare the observed peptide masses to the in silico tryptic digest of human TRPM8 (UniProtKB - Q7Z2W7). Of all the peptides found to match

TRPM8, 8% displayed unique peptide fragments with a mass error below 13.0 ppm (for one example, see Figure S1(A)).

The filtered raw data with a charge of +2 to +4 and with a mass to charge ratio of 200–1900 were used for protein identification using OMSSA algorithm[55] with the avail of SearchGUI 3.3.17[56] and Peptide Shaker 1.16.44[57] open-source interface software. Peptide and protein identifications were obtained by searching against a human Uniprot proteome database (UP000005640). The false discovery rate was set to 1%. TRPM8 protein (Uniprot Q7Z2W7) was identified with a 100% confidence, with 4 identified peptides displaying a spectra of unique peptide fragments (for one example see Figure S1(B)).

2.13 | Statistical analysis and data preparation

Preparation of data for figures was done using R Studio version 3.4.4 and GraphPad Prism version 7.

Statistical analysis of non-RNA seq data was done using Graph-Pad Prism version 7. To compare 2 groups of data: paired T tests or Wilcoxon signed rank tests were used for paired normally and non-normally distributed data, respectively; Mann–Whitney tests were used for unpaired, non-normally distributed data sets. To compare more than 2 groups of data: Freidman tests (with Dunn's multiple comparison test) was used for paired, non-normally distributed data; one-way ANOVA (with Holm Sidak's multiple comparison test) or Kruskal–Wallis (with Dunn's multiple comparison test) were used for unpaired, normally and non-normally distributed data sets, respectively. A two-way ANOVA was used to compare time/treatment interactions.

3 | RESULTS

3.1 | TRPM8 is expressed in cells of the monocyte/macrophage lineage in humans

Previous data have demonstrated expression of TRPM8 in murine peritoneal macrophages[45]; therefore, we first sought to determine whether cells of the human monocyte/macrophage lineage express TRPM8. Antibody staining of human blood CD14$^+$ monocytes and in macrophages derived from them in vitro (Mo-M) revealed similar levels of TRPM8 expression in both cell populations, albeit at lower levels than in the prostate cancer cell line, DU145, which has previously been reported to express TRPM8[58] (Figures 1(A) and 1(B)). Conversely, assessment of TRPM8 RNA expression in the same cell populations using quantitative real-time PCR analysis revealed detectable expression of *TRPM8* in Mo-M, but not in their CD14$^+$ monocyte precursors (Figure 1(C)). In line with this, analysis of published RNA seq data[59] also indicated the absence of *TRPM8* in human primary monocytes. Given this apparent disassociation between the expression of TRPM8 RNA and protein, we sought to substantiate the results of our antibody staining of blood monocytes by using a shotgun proteomics approach. To this end, delipidated and trypsinized membrane fractions of CD14$^+$ monocytes were analyzed by high-resolution mass
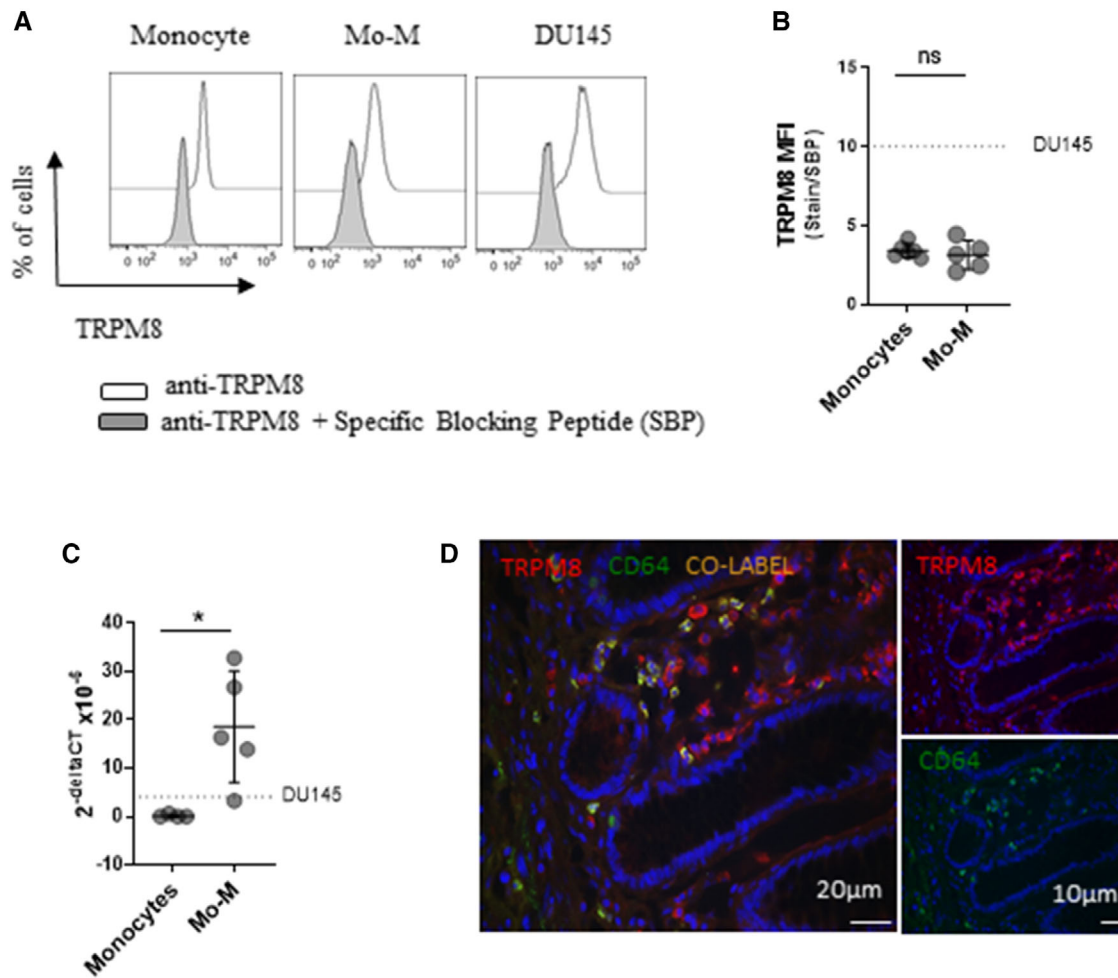
FIGURE 1 TRPM8 is expressed in cells of the monocyte/macrophage lineage in humans. (A)–(C) Peripheral blood monocytes were cultured for 6 days in the presence of M-CSF to obtain Mo-M. The TRPM8-expressing DU145 cell line was used as a positive control. (A) and (B) Flow cytometry analysis showing TRPM8 protein expression in permeabilized cells after staining with anti-TRPM8 antibody alone or in combination with a specific blocking peptide (SBP). (A) Representative plots and (B) mean fluorescence intensity (MFI) of TRPM8 protein expression presented as a fold change compared with SBP control. (C) Quantitative real time PCR analysis showing TRPM8 RNA expression. Data are expressed as $2^{-\Delta CT}$ by normalization to GAPDH. (B) and (C) Each dot represents data from an independent donor. Mean $\pm$ SD are indicated. $*$ = $p < 0.05$, ns = $p > 0.05$ (Mann–Whitney). Dotted line = value from DU145 cell line (mean of 3 independent passages). (D) Representative immunohistochemistry image showing costaining (yellow) of TRPM8 (red) and CD64 (green) in inflamed human colonic mucosa

spectrometry. The analysis provided positive identification of the TRPM8 protein (for details see *Materials and Methods* and Figures S1(A) and S1(B)), therefore indicating that human CD14$^+$ monocytes do indeed express TRPM8 protein despite the lack of detectable RNA. Finally, we used tissue from the human intestine, one of the locations where macrophages are derived from blood monocytes under both steady-state and inflamed conditions,[9] in order to investigate TRPM8 expression in a tissue-resident monocyte/macrophage population. Consistent with expression of TRPM8 in blood monocytes and in in vitro-derived macrophages, immunohistochemistry staining revealed that a sizeable fraction of TRPM8$^+$ cells the inflamed colonic mucosa costained for CD64 (Figure 1(D)). The TRPM8$^+$ cells that are CD64$^-$ likely represent other lamina propria cells such as dendritic cells, which characteristically lack CD64 expression in the intestinal mucosa[60] or lymphocytes. Together, these data confirm that

TRPM8 is expressed in cells of the monocyte/macrophage lineage in humans.

3.2 | Pharmacologic inhibition of TRPM8 alters plasma membrane potential in differentiating human monocytes

TRPM8 is a cation channel with the primary capacity to alter membrane potential. To investigate the functionality of TRPM8 expressed by human monocytes, we examined the plasma membrane potential of cells cultured in the presence of well-characterized pharmacologic modulators of TRPM8 activity. Specifically, we used the voltage-sensitive dye DiSBAC$_2$3, which exhibits enhanced fluorescence output in depolarized cells.[61,62] Human blood CD14$^+$ monocytes were

cultured in M-CSF to initiate their transition into Mo-M and at the same time exposed to either 10 μM icilin (a TRPM8 agonist),[30] 10 μM AMTB (a TRPM8 antagonist),[63] or DMSO (vehicle control). Membrane potential was then assessed over a 3-h time frame, using 100 ng/ml PMA as a positive control for cell depolarization. We observed no measurable change in membrane potential when TRPM8 was exposed to icilin over this time frame, but surprisingly exposure to AMTB resulted in progressive depolarization of the monocyte plasma membrane that became most obvious after 3 h of culture (Figures 2(A) and 2(B)) and was still evident 24 h later (Figures 2(C) and 2(D)). Importantly, similar results were obtained using an alternative TRPM8 antagonist, M8-B,[64] and agonist, M8-Ag[65] (Figure S2(A)). The capacity of the TRPM8 antagonists and not the agonists to alter membrane potential implies that there is endogenous activity of TRPM8 in monocytes, which the antagonists are able to inhibit. The reason for depolarization, rather than hyperpolarization of the plasma membrane following inhibition of channel activity is unknown, but could reflect an internal localization of TRPM8,[66] or the capacity of it to regulate other ion channels.[67]

3.3 | TRPM8 antagonism promotes inflammatory capacity in the early stages of monocyte to macrophage differentiation

Alterations in membrane potential have been reported to significantly alter cell behavior, survival, and differentiation[62,68]; therefore, we next examined the functional consequences of TRPM8 inhibition in differentiating human monocytes. To this end, blood CD14+ monocytes were cultured with M-CSF in the presence or absence of AMTB. Cell viability and surface expression of CD14 were assessed by flow cytometry at 3 and 24 h. Although no phenotypic alterations were observed after 3 h (Figures S2(B) and S2(C)), we observed a striking increase in the % of viable monocytes cultured in the presence of AMTB after 24 h, compared with control cells cultured in vehicle alone (Figures 3(A) and 3(B)). AMTB treatment also led to an increase in the % and number of CD14+ cells within the viable monocyte fraction (Figures 3(C)–3(E)). These CD14+ cells were reminiscent of the precultured monocyte population in terms of their level of CD14 but had acquired expression of CD16 (Figure S2(D)). The CD14− fraction lacked CD16 but were bona fide monocytes as indicated by their expression of HLA-DR and CD64 (Figure S2(D)).

A major function of monocytes is to sense and respond to bacterial products, so we next assessed whether TRPM8 activity in monocytes might affect their response to LPS. Blood CD14+ monocytes that had been cultured for 24 h with M-CSF in the presence or absence of AMTB were exposed to LPS for the final 3 h and then analyzed by intracellular flow cytometry staining for TNFα. We found that under both conditions, TNFα was produced exclusively by the CD14+ population (Figure 3(F)). In line with the increased % of CD14+ cells in AMTB-treated cultures, we observed that cells cultured with AMTB contained a significantly greater proportion of TNFα-producing cells than control cells (Figures 3(F) and 3(G)). No TNFα was produced in the absence of LPS exposure indicating that AMTB treatment does not directly trig-

ger TNFα production by monocytes (Figure 3(F)). Similar results were obtained using the alternative TRPM8 antagonist, M8-B, and culture in the presence of 2 independent agonists, icilin and M8-Ag, had no effect on cell survival, the proportion of CD14+ cells, or LPS-driven TNFα production (Figures S2(E)–S2(G)). These data suggest that TRPM8 activity in differentiating blood CD14+ monocytes acts to limit cell survival and inflammatory capacity in the early stages of their differentiation to macrophages.

To establish whether this susceptibility to TRPM8 activity blockade was also a feature of monocyte-derived cells in human tissue, we isolated LPMCs from endoscopic colonic biopsies and exposed them to AMTB in an overnight culture. We found, in keeping with the blood monocyte data, that following a 3-h LPS stimulation, a fraction of CD14+ cells within the CD45+ CD64+ HLA-DR+ FSChi population of LPMCs was TNFα+ and that AMTB-treated LPMCs contained a significantly higher proportion of these TNFα-producing cells (Figures 4(A) and 4(B)). Together, these data indicate that TRPM8 activity acts to reduce inflammatory potential in human tissue as well as blood CD14+ monocytes.

3.4 | TRPM8 antagonism results in an impaired ability of monocytes to differentiate into macrophages

Given the impact of TRPM8 antagonism on human monocyte survival and inflammatory properties in the early stages of their transition to macrophages, we were intrigued to explore the longer term consequences of TRPM8 activity on monocyte cell fate. For this purpose, human CD14+ blood monocytes were differentiated into Mo-M for 6 days in the presence or absence of AMTB. Consistent with the short-term effect of TRPM8 antagonism on monocyte cell survival, we found a significantly greater proportion and number of live Mo-M when cells had been differentiated in the presence of AMTB compared with control cell cultures (Figures S3(A)–S3(C)). Unlike the 24 h time point, Mo-M were all CD14+ (data not shown) and no increase in LPS-induced TNFα production was observed in AMTB-differentiated cells (Figure S3(D)).

One of the principal functions of macrophages is phagocytosis, a process crucial for the immune response to pathogens, as well as in tissue homeostasis and remodeling. To investigate the phagocytic capacity of Mo-M and their monocyte precursors, we assessed the uptake of 2 μm fluorescent carboxylate microspheres by comparing fluorescence at 37°C with that at 4°C when active uptake is inhibited. Fluorescent Mo-M were

present at 37°C, but mostly absent at 4°C indicating that these cells are capable of temperature-dependent phagocytosis (Figures S3(E) and S3(F)). In contrast, fluorescent monocytes were detected at both 37°C and 4°C suggesting that unlike their Mo-M derivatives, monocytes are weakly phagocytic, although they have some capacity for surface binding of the microspheres (Figures S3(E) and S3(G)). We next examined phagocytosis in Mo-M that had been differentiated from CD14+ monocytes in the presence or absence of AMTB.
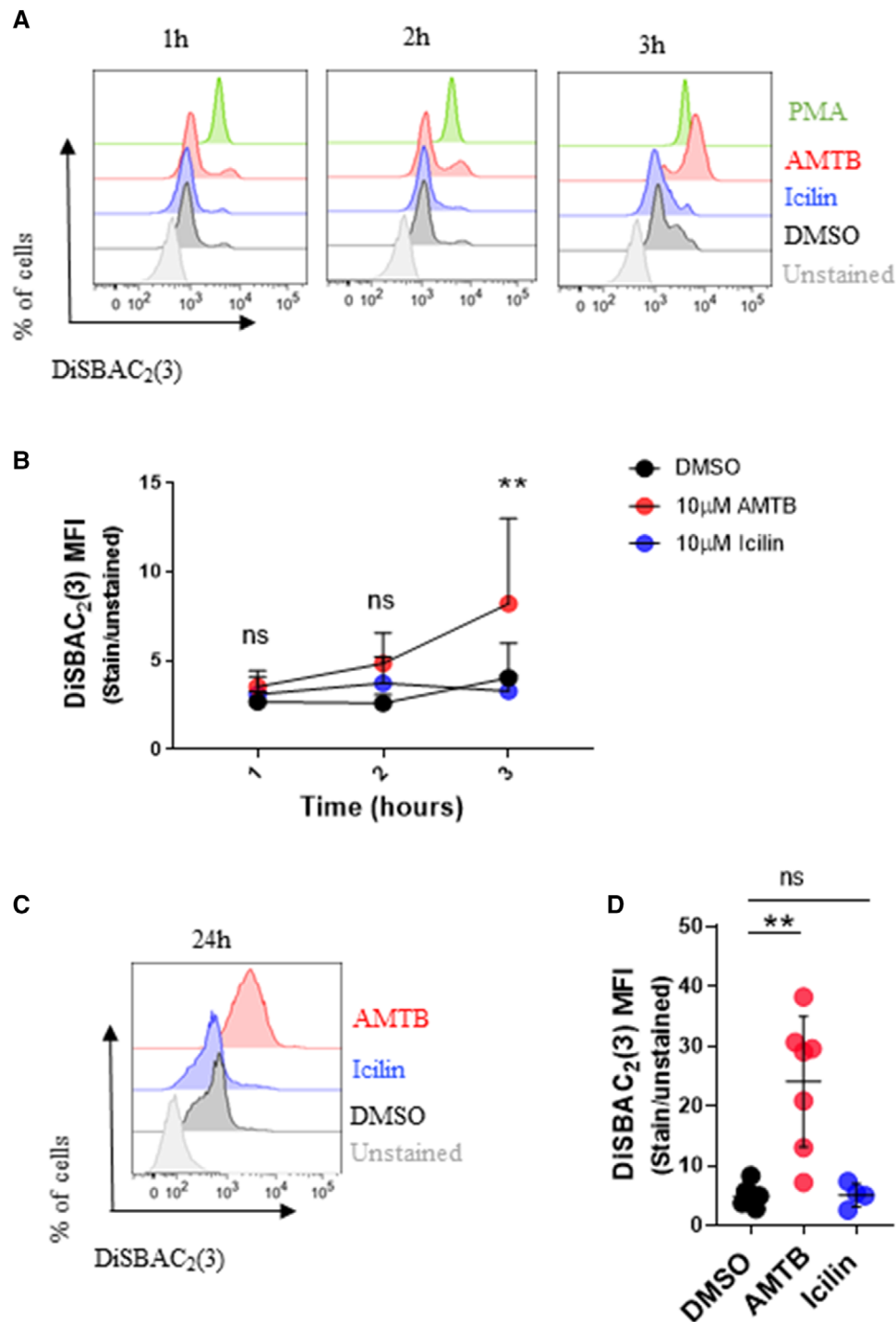
FIGURE 2　Pharmacologic inhibition of TRPM8 alters plasma membrane potential in differentiating human monocytes. Peripheral blood CD14+ monocytes were cultured with M-CSF in the presence of 10 μM icilin, 10 μM AMTB, 10 μg/ml PMA, or DMSO for 1, 2, 3, and 24 h. Cells were then stained with 1 μM DiSBAC$_2$(3) and analyzed by flow cytometry to measure membrane potential. (A) Representative plots and (B) MFI (mean + SD of 4 independent donors) of DiSBAC$_2$(3) staining at 1, 2, and 3 h. 2-Way ANOVA with Dunnett's multiple comparisons test. (C) Representative plot and (D) MFI of DiSBAC$_2$(3) staining at 24 h. Each dot represents an independent donor. Mean ± SD are indicated. Kruskal–Wallis test with Dunn's multiple comparisons. MFI = mean fluorescence intensity (fold change above unstained sample). ** = $p < 0.01$, ns = $p > 0.05$
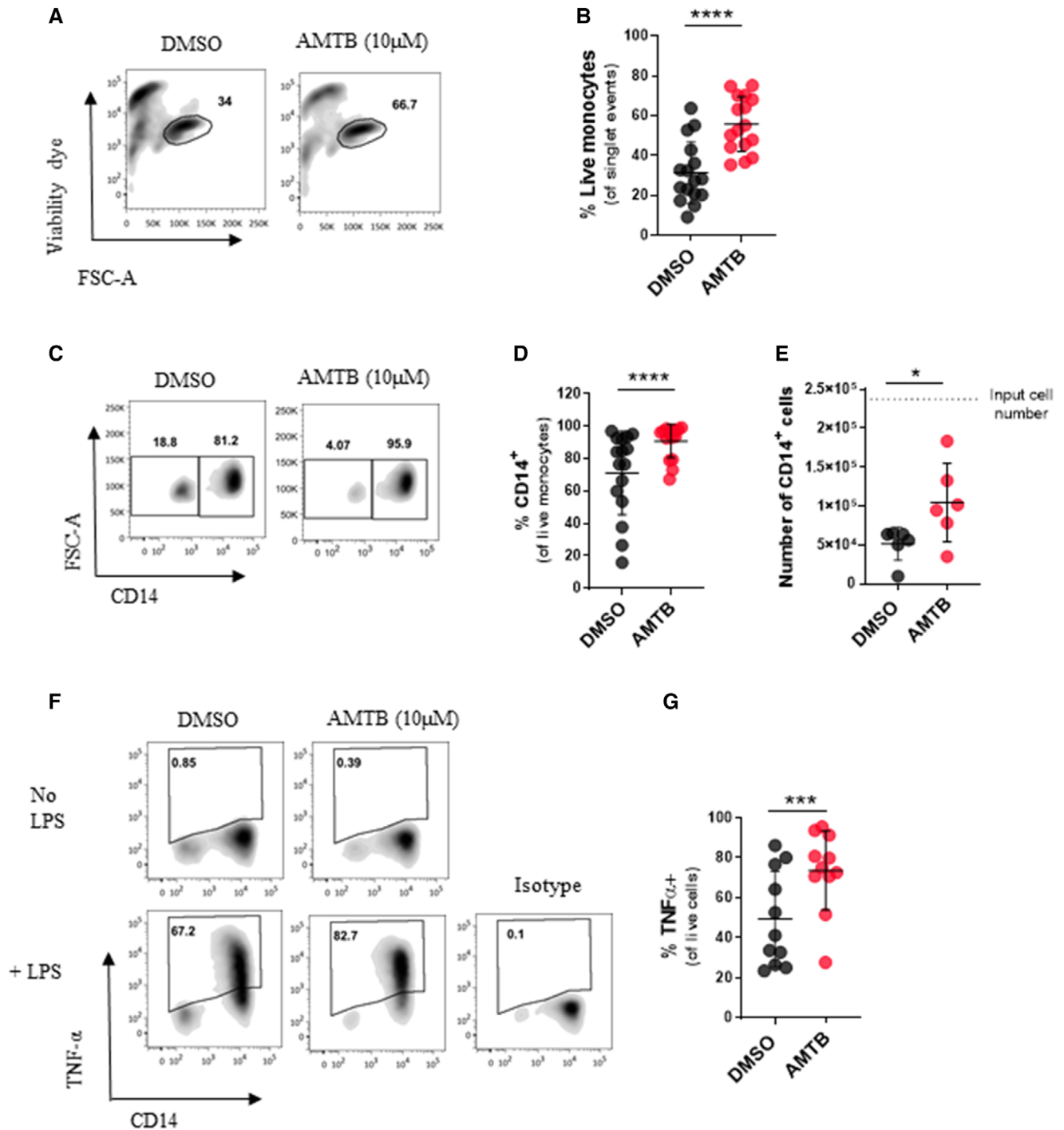
FIGURE 3 TRPM8 antagonism promotes inflammatory capacity in the early stages of monocyte to macrophage differentiation. Peripheral blood CD14$^+$ monocytes were cultured with M-CSF in the presence of 10 μM AMTB or DMSO and then analyzed by flow cytometry staining at 24 h. (A) Representative plots and (B) summary data showing % of live monocytes. (C) Representative plots showing CD14 staining, (D) % and (E) absolute number of CD14$^+$ cells. Input cell number is indicated as a dotted line. (F) Representative plots and (G) % TNFα^+ cells measured by intracellular staining after a 3 h stimulation with 100 ng/ml LPS, in the presence of 3 μM monensin. Each dot represents data from 1 independent donor. Mean $\pm$ SD are indicated. (B) Paired t test. (D), (E), and (G) Wilcoxon signed-rank test. * = $p < 0.05$, *** = $p < 0.001$, **** = $p < 0.0001$
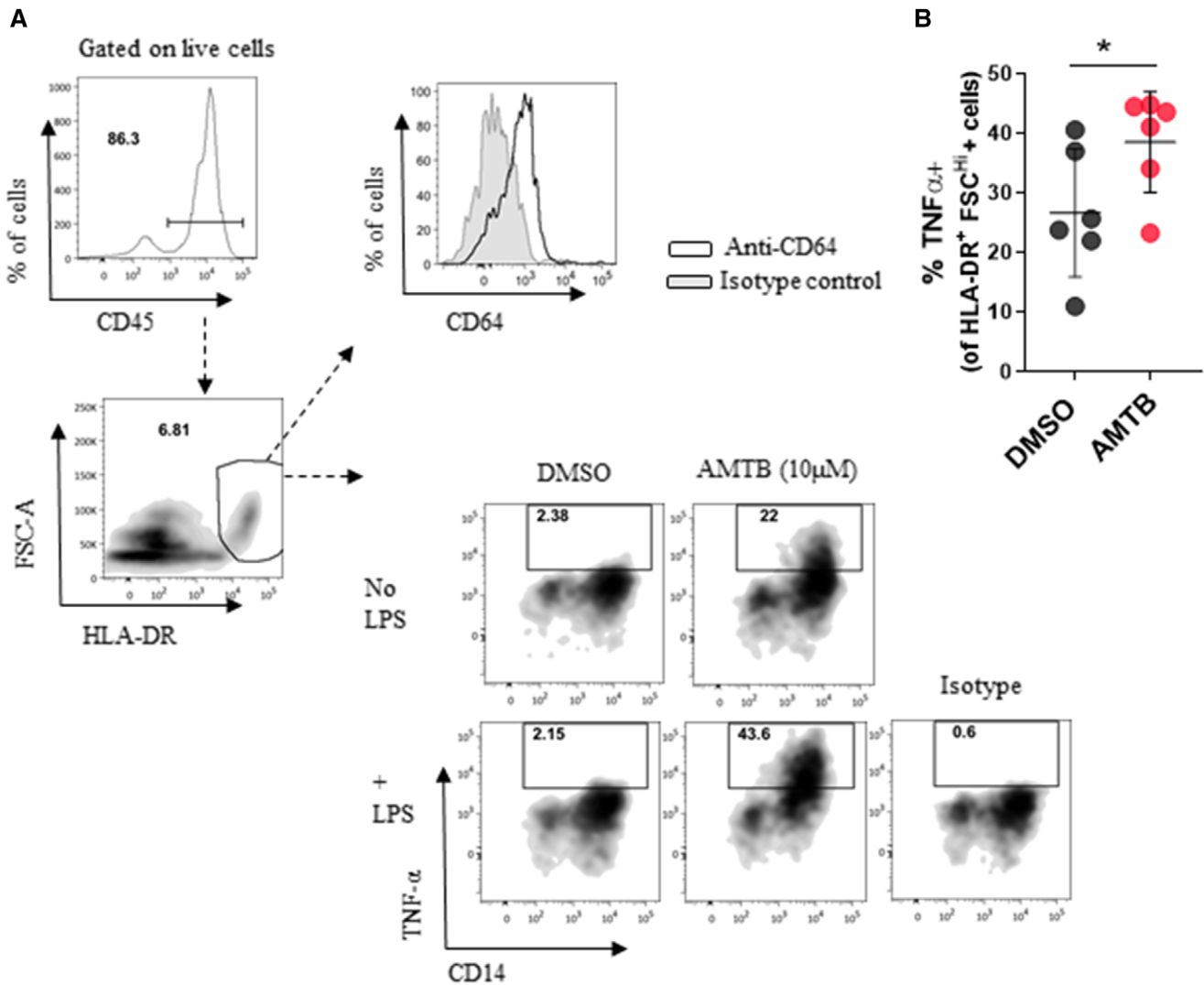
FIGURE 4 TRPM8 antagonism promotes inflammatory capacity in lamina propria monocytes. Lamina propria mononuclear cells (LPMCs) were isolated from endoscopic colonic biopsies and cultured overnight with 10 μM AMTB or DMSO. (A) Representative flow cytometry plots to show the gating of monocyte/macrophage cells. (B) % TNFα^+ cells measured by intracellular staining after stimulation with 100 ng/ml LPS, in the presence of 3 μM monensin, for the final 3 h of culture. Each dot represents data from 1 independent donor. Mean $\pm$ SD are indicated. Wilcoxon signed-rank test. $^* = p < 0.05$

AMTB-differentiated Mo-M had impaired phagocytic capability, as shown by a reduction in the proportion of cells that had taken up microspheres, as well as a reduction in the number of microspheres taken up per cell (mean fluorescence intensity [MFI]) (Figures 5(A)–5(C)). Addition of AMTB to Mo-M that had developed normally in the absence of AMTB, at the same time as the microspheres did not lead to any change in phagocytic activity, implying that TRPM8 activity is required for normal monocyte to macrophage cell differentiation rather than being directly required during phagocytosis itself (Figures S3(H) and S3(I)). Uptake of the soluble sugar FITC dextran was also reduced in AMTB-differentiated Mo-M suggesting that AMTB has broader effects on other endocytic mechanisms in addition to the uptake of large particles by phagocytosis (Figures S3(J) and S3(K)).

To further investigate the role of TRPM8 activity in normal monocyte to macrophage differentiation, we examined the transcriptional profiles of undifferentiated CD14$^+$ blood monocytes and Mo-M differentiated with M-CSF in the presence of DMSO or AMTB (Mo-M DMSO and Mo-M AMTB, respectively) using RNA-seq. We first sought to characterize the transcriptional changes that occur normally in M-CSF-driven monocyte to macrophage differentiation and therefore compared gene expression in the CD14$^+$ monocyte and Mo-M-DMSO samples. This revealed that 3109 genes (26.6% of expressed genes) were significantly down-regulated (*Diff-DOWN*) and 3403 genes (29.1% of expressed genes) were significantly up-regulated (*Diff-UP*) in this process (Figures 5(D) and S4), fitting with major changes in cellular function and phenotype between monocytes and macrophages. Having identified the normal transcriptional changes during Mo-M differentiation, we next asked whether there were significant differences in the gene expression profiles of Mo-M differentiated in the presence of DMSO or AMTB. Principal component analysis showed a clear
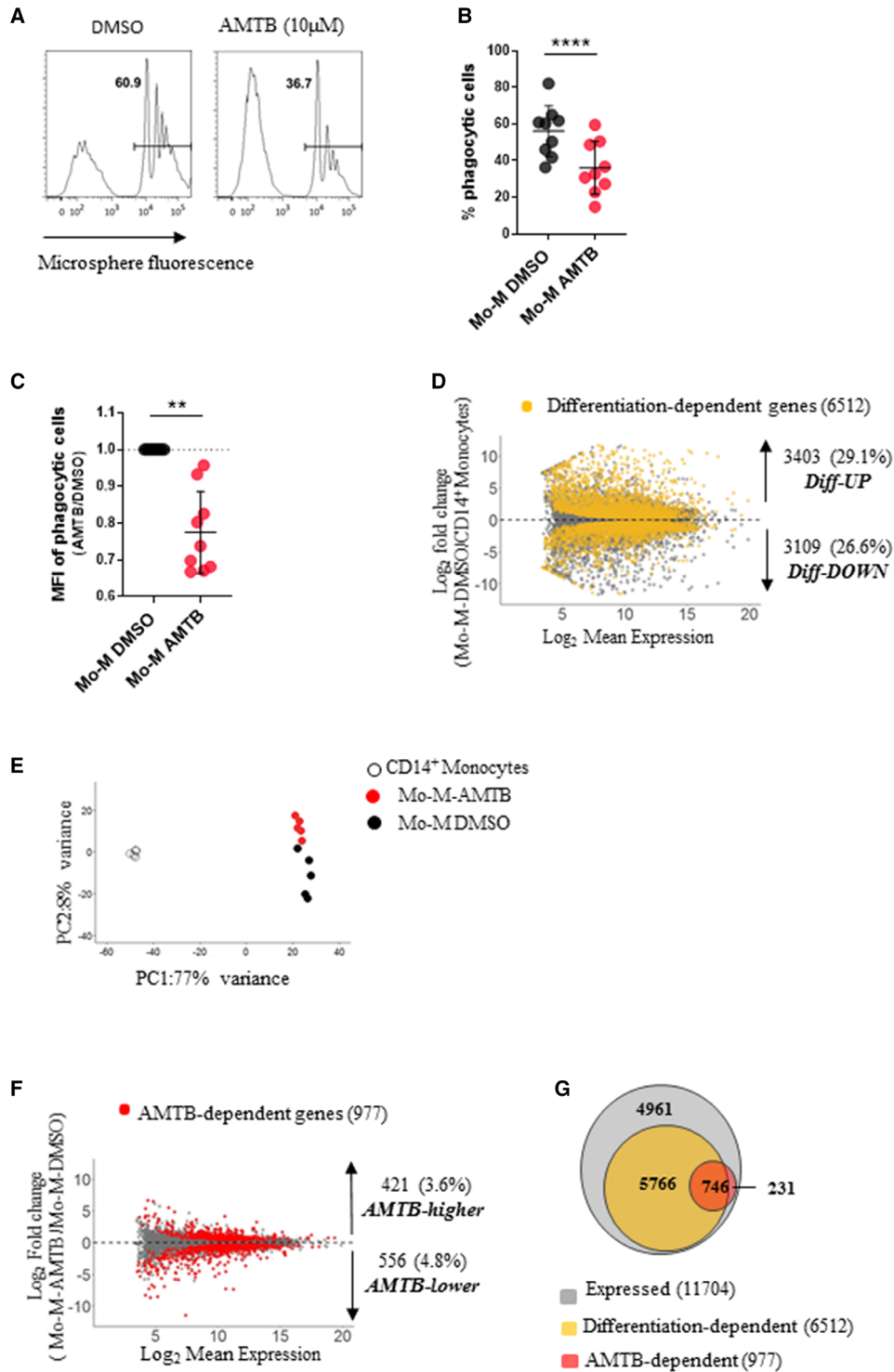
FIGURE 5 Macrophages derived from monocytes in the absence of TRPM8 activity are functionally and transcriptionally distinct. Peripheral blood CD14$^+$ monocytes were differentiated into Mo-M by 6 days of culture with M-CSF in the presence of either 10 μM AMTB (Mo-M AMTB) or DMSO (Mo-M DMSO). (A)–(C) Mo-M DMSO or Mo-M AMTB were incubated with 2 μm fluorescent microspheres for 1.5 h at 37°C and then analyzed by flow cytometry. (A) Representative plots, (B) %, and (C) MFI (fold change compared DMSO control) of phagocytic cells. Each dot represents an independent donor. Mean $\pm$ SD are indicated. (B) Paired t test, (C) Wilcoxon signed-rank test. **** = $p < 0.0001$, ** = $p < 0.01$. (D)–(G) RNA-seq analysis on CD14$^+$ monocytes, Mo-M AMTB, and Mo-M DMSO from 5 independent donors. (D) MA plot showing log$_2$ fold change in gene expression in CD14$^+$ monocyte versus Mo-M DMSO samples. Genes differentially expressed are defined as differentiation-dependent genes (padj = < 0.05). Number and % of genes are indicated. (E) Principal component analysis. (F) MA plot showing log$_2$ fold change in gene expression in Mo-M AMTB versus Mo-M DMSO samples. Genes differentially expressed are defined as AMTB-dependent genes (padj = < 0.05). Number and % of genes are indicated. (G) Venn diagram (http://biovenn.nl) to show the proportional overlap between expressed, differentiation-dependent, and AMTB-dependent genes. Numbers of genes are indicated

segregation of the Mo-M DMSO and Mo-M AMTB transcriptomes (Figure 5(E)). Indeed, when we performed differential gene expression analysis, we identified 556 and 421 genes that were significantly lower and higher in Mo-M AMTB compared with Mo-M DMSO, respectively (hereafter referred to as *AMTB-lower* and *AMTB-higher*) (Figure 5(F)). Comparison of the AMTB-dependent and differentiation-dependent gene sets revealed that the majority of AMTB-dependent genes (746/977) were also affected by differentiation (Figure 5(G)), indicating a notable effect of TRPM8 antagonism on the differentiation of monocytes to macrophages. Upon further interrogation, we found that the majority of the *AMTB-higher* genes were normally down-regulated during differentiation (253/421 genes) and that the majority of *AMTB-lower* genes were normally up-regulated (331/556 genes) (Figures 6(A)–6(D)), suggesting that TRPM8 antagonism predominantly acts to inhibit aspects of the differentiation programme.

GO enrichment analysis of the *AMTB-higher/Diff-DOWN* and *AMTB-lower/Diff-UP* genes revealed that AMTB blocked the down-regulation of genes involved in "positive regulation of catabolic process" and "Notch signaling pathway" in addition to preventing the up-regulation of genes involved in "chemotaxis" and "external encapsulating structure organization," among others (Figures 6(E) and 6(F)). The GO terms that were most significantly enriched in the minority of genes that did not follow this pattern were "carbohydrate transport" (*AMTB-higher/Diff-UP*), "defense response to Gram-positive bacterium" (*AMTB-higher/Diff-NO CHANGE*), "defense response to bacterium" (*AMTB-lower/Diff-DOWN*), "cell-substrate adhesion" (*AMTB-lower/Diff-NO CHANGE*) (Figures 6(E) and 6(F)). Five phagocytosis and 3 endocytosis GO terms were significantly enriched within the AMTB-dependent gene lists; all of which were enriched within the *AMTB-lower/Diff-UP* gene set fitting with our observation that AMTB results in a defect in phagocytic and endocytic mechanisms (Figure S5).

Collectively these data show that TRPM8 antagonism results in an impaired ability of monocytes to differentiate into macrophages, suggesting that TRPM8 activity acts to promote aspects of this differentiation programme.

3.5 | TRPM8 antagonism within a critical time window is necessary to promote monocyte survival and inflammatory capacity

We had so far established that antagonism of TRPM8 activity influences the survival and inflammatory capacity of human monocytes and has longer term effects on their ability to differentiate into macrophages. It was however unclear at what stage of Mo-M differentiation, TRPM8 activity was most important. We had shown that exposure of human CD14$^+$ monocytes to AMTB results in progressive membrane depolarization that commenced after the first 3 h of culture and therefore went on to investigate whether blockade of TRPM8 activity in this early time frame was sufficient to drive downstream phenotypic and functional effects. Human CD14$^+$ monocytes were cultured with M-CSF plus AMTB for 3 h and then washed into fresh medium with M-CSF only for further differentiation (0–3 h; Figure 7(A)). In par-

allel experiments, AMTB was added to differentiating CD14$^+$ monocytes after the first 3 h and left in for the remaining culture period (3–24 h/6d; Figure 7(A)), or was added for the whole culture period (0–24 h/6d; Figure 7(A)). When all experimental systems were examined at 24 h, we found that exposing the cells to AMTB for only the first 3 h of culture (0–3 h) or for all of the culture period (0–24 h) elicited a similar effect on cell survival, percentage of CD14$^+$ cells, and LPS-driven TNFα production (Figures 7(B)–7(D)). In contrast, delaying AMTB exposure until after the initial 3 h of culture (3–24 h) resulted in a significantly reduced effect on cell survival, percentage of CD14$^+$ cells, and LPS-driven TNFα production (Figures 7(B)–7(D)).

To investigate the longer term consequences of this TRPM8-sensitive time window, we examined the Mo-M 6 days later. In line with the effects we observed on monocyte cell behaviour and function at 24 h, exposing cells to AMTB for the first 3 h only (0–3 h) elicited a similar increase in cell survival to when AMTB was continually present (0–6 d), and adding in AMTB after this period led to a significantly reduced effect on cell survival (Figure 7(E)). Exposure to AMTB for the first 3 h of culture only (0–3 h) was also sufficient to limit the phagocytic capacity of the Mo-M 6 days later, but this effect was less pronounced than when AMTB was continually present (0–6 d). Furthermore, delaying AMTB addition until after this 3-h period was equally as effective in reducing phagocytic capacity (Figures 7(F) and 7(G)). TRPM8 activity therefore appears to have 2 distinct phases of action. Initially, TRPM8 activity in the first 3 h is necessary to limit cell survival and inflammatory capacity during the early stages of monocyte to macrophage differentiation (i.e., first 24 h). Intriguingly, the influence of TRPM8 activity in these first 3 h can be at least partially maintained even after 6 days. However, the more pronounced differentiation effects mediated by TRPM8 activity (i.e., reduced phagocytic capacity of Mo-M) are linked to later stages of the differentiation process.

4 | DISCUSSION

Monocytes are integral components of the immune response to pathogens and also contribute to the pathogenesis of conditions such as atherosclerosis, inflammatory disease, and cancer. They are highly plastic cells but the regulation of their diverse developmental trajectories is poorly understood. A role for TRPM8 in immune regulation has recently come to light in a series of observations focusing on its control of immune responses in the intestine[45,47,48] and its functional expression by murine peritoneal macrophages[45] and T cells.[46] We have for the first time demonstrated that TRPM8 acts to facilitate the transition of human CD14$^+$ monocytes to macrophages. In vitro inhibition of TRPM8 predominantly acted to oppose the up- and down-regulation of a subset of differentiation-dependent genes. Functionally, this resulted in enhanced survival and LPS-induced TNFα production in the early stages and impaired phagocytic activity in the later stages of differentiation.

TRPM8-mediated control of monocyte to macrophage transition may have particular relevance in the intestine where many of the tissue-resident macrophages are continually replenished by blood
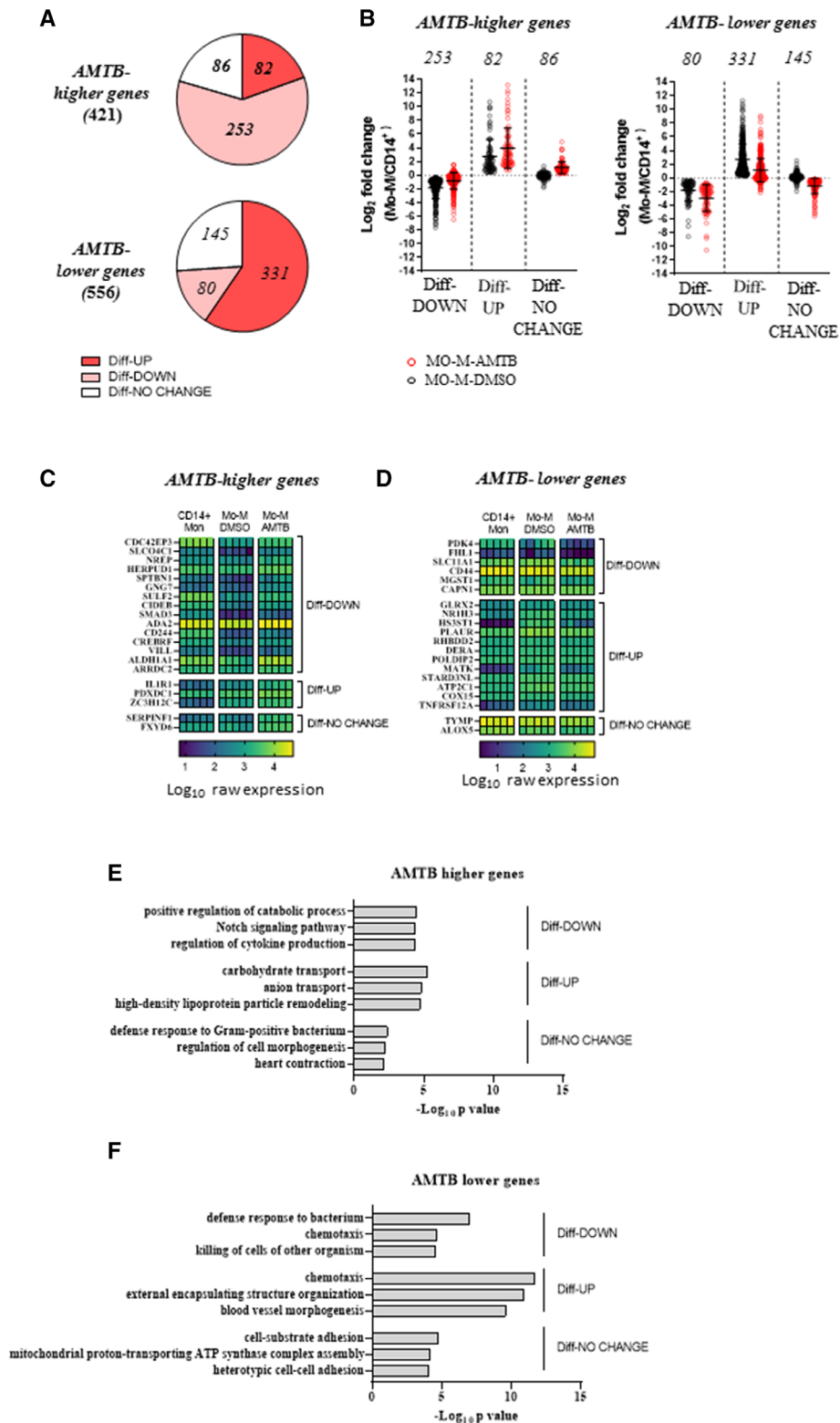
FIGURE 6 Antagonism of TRPM8 activity limits aspects of monocyte to macrophage differentiation. Analysis of the AMTB-dependent genes identified in the RNA-seq analysis. (A) Pie charts show the numbers of *AMTB-higher* and *AMTB-lower* genes that are up-regulated (*Diff-UP*), down-regulated (*Diff-DOWN*), or unchanged (*Diff-NO CHANGE*) by differentiation. (B) Graphs show $\log_2$ fold change in gene expression in CD14^{+} monocytes versus Mo-M DMSO samples (black circles) or Mo-M AMTB samples (red circles) for *AMTB-higher* and *-lower* genes. Genes are divided into clusters according to their response to differentiation. Numbers of genes per cluster are indicated. (C) and (D) Individual donor $\log_{10}$ expression levels of the top 20 *AMTB-higher* and *-lower* genes, respectively (divided based on response to differentiation). (E) and (F) Gene enrichment analysis showing the top 3 significantly enriched gene ontology terms (http://metascape.org) in the *AMTB-higher* and *-lower* gene sets, respectively
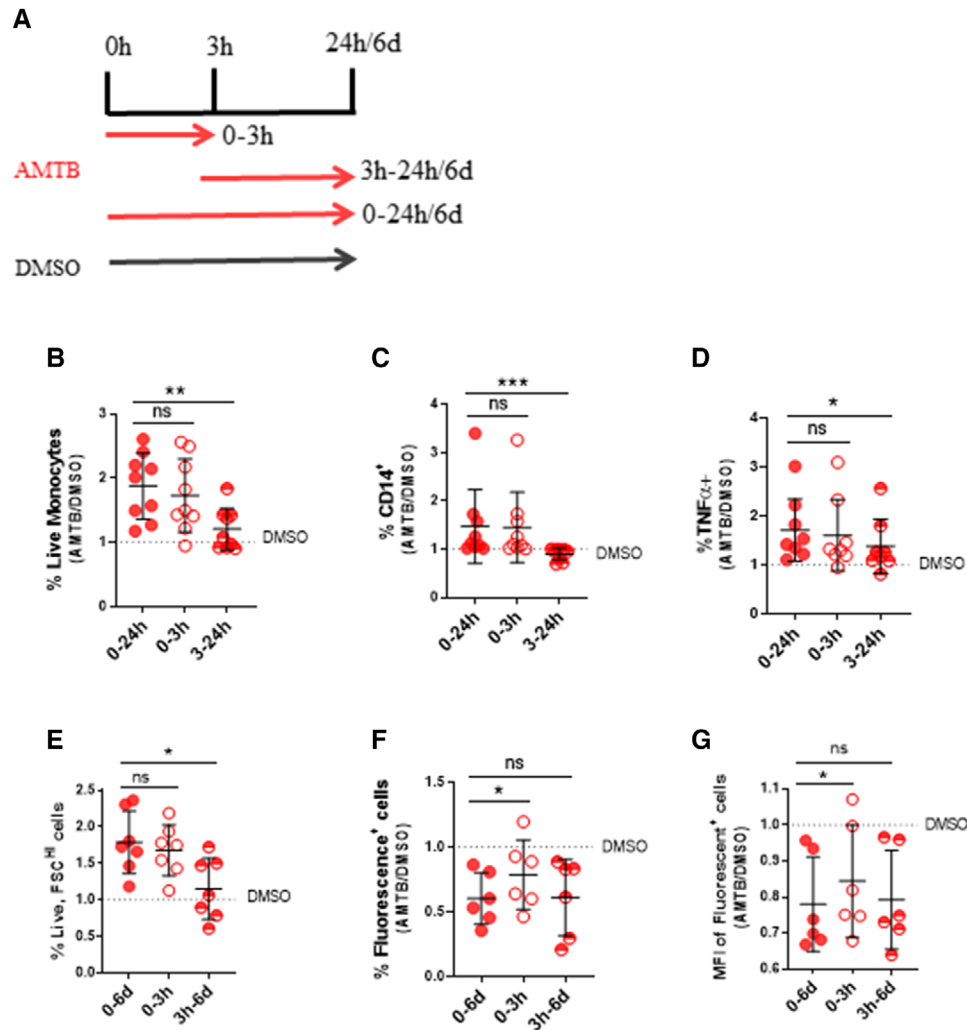
FIGURE 7 TRPM8 antagonism within a critical time window is necessary to promote monocyte survival and inflammatory capacity. Peripheral blood CD14$^+$ monocytes were cultured with M-CSF for 24 h or 6 days. 10 μM AMTB was added either for the first 3 h of differentiation and then washed out for the remaining culture period (0–3 h), or from 3 h after the initiation of culture until the end of the differentiation period (3–24 h or 3 h–6d). Control cells were exposed to AMTB or DMSO for the whole culture period (0–24 h or 0 h–6d). Cells were then analyzed by flow cytometry at (B)–(D) 24 h or (E)–(G) 6 days. (A) Illustration of the experimental set-up. (B) % of live cells as a proportion of singlet events. (C) % of CD14$^+$ cells as a proportion of live events. (D) % of TNFα^+ cells measured by intracellular staining following stimulation for 3 h with 100 ng/ml LPS. (E) % of live, FSC^{hi} as a proportion of singlet events. (F) % and (G) MFI of phagocytic cells following incubation of Mo-M with fluorescent microspheres. Measurements are expressed as a fold change compared with the DMSO control (dotted line). Each dot represents data from an independent donor. Mean $\pm$ SD are indicated. (B) One-way ANOVA with Dunnett's multiple comparisons test, (C)–(E): Friedman's with Dunn's multiple comparisons test) * = $p < 0.05$, ** = $p < 0.01$, *** = $p < 0.001$

monocytes[9] and hallmark features of monocyte to macrophage differentiation include the acquisition of phagocytic properties and downregulation of proinflammatory responses to bacterial products.[9,69] Abnormal differentiation of intestinal monocytes during inflammation leads to the accumulation of cells that are hyper-responsive to bacterial stimulation and produce potent inflammatory mediators including TNFα.[70,71] Indeed, we found that intestinal as well as blood-derived CD14$^+$ monocytes were susceptible to effects of TRPM8 activity blockade.

Our observation that TRPM8 inhibition in differentiating CD14$^+$ monocytes enhanced LPS-induced TNFα production is in keeping with the hyperinflammatory phenotype previously observed in peritoneal

macrophages,[45] and CD11c$^+$ splenocytes[47] derived from TRPM8-deficient mice. Although de Jong et al.[47] attributed this phenotype to lack of the immunosuppressive neuropeptide CGRP release from mucosal sensory neurons in TRPM8 knockout mice rather than a direct effect of TRPM8 activity in CD11c$^+$ cells, Khalil et al.[45] proposed an intrinsic effect of TRPM8 activity on the function of peritoneal macrophages. Unlike Khalil et al.,[45] who observed responses to the TRPM8 agonist, menthol, in wild-type, but not TRPM8-deficient peritoneal macrophages, we observed no measurable effect of 2 independent agonists, icilin and M8-Ag, on CD14$^+$ monocytes, despite their strong susceptibility to TRPM8 antagonism. In keeping with this, another report noted the absence of icilin-induced currents in primary

human CD14$^+$ monocytes using patch clamp analysis.[72] One possible explanation for the absence of TRPM8 agonist effects in human CD14$^+$ monocytes is that TRPM8 may already be maximally active in these cells, and this raises the interesting possibility of differential levels of endogenous TRPM8 activity in different cellular contexts. Indeed, the mechanisms that maintain endogenous activity of TRPM8 in human monocytes is an important area for future study. Our experiments were all performed at 37°C, higher than the temperature range likely to activate TRPM8 (<28°C), suggesting that factors other than temperature are at play. TRPM8 is polymodally activated by both cell intrinsic and extrinsic factors. Extrinsic factors include hormone derivatives,[37,39] which would be present in the FBS used in our experiments. Despite this, we have observed similar effects of the TRPM8 antagonist in preliminary experiments performed in serum-free medium, in addition to cultures polarized with GM-CSF alone or in combination with IL-4 (data not shown), indicating that the endogenous activity of TRPM8 in monocytes is not solely dependent on serum components or specific for a particular cytokine exposure. It is also plausible that endogenous activity of TRPM8 in monocytes is due to cell intrinsic factors such as the integral membrane phospholipid, PI(4,5)P$_2$.[33]

We observed that inhibition of TRPM8 activity in primary human CD14$^+$ monocytes led to progressive and sustained depolarization of the plasma membrane, as measured by the dye, DiSBAC$_2$(3). This was a surprising finding given that activation of TRPM8 classically leads to the influx of cations, predominantly calcium, leading to cell depolarization.[30] Under this view, blockade of activity would lead to cell hyperpolarization rather than depolarization. Further work would be required to determine whether this effect reflects the localization of the channel; for example, in an intracellular vesicle where inhibition of the channel may result in accumulation of calcium within the cytoplasm.[73] Alternatively, inhibition of TRPM8 activity could influence local calcium signaling, which could subsequently regulate other voltage-gated channels to control plasma membrane potential.[74,75]

AMTB, the main TRPM8 antagonist used in our experiments, has been identified as a specific and selective antagonist of TRPM8.[63] Although there is a more recent report describing an off-target effect of AMTB on voltage-gated sodium channels,[76] we were unable to replicate the effects of AMTB on human monocytes with the prototypical voltage-gated sodium channels inhibitor lidocaine, demonstrating that this activity is unlikely to be responsible for the effects we see (data not shown). In addition, we did not only rely on one agent to draw our conclusions; an independent antagonist, M8-B, was utilized and it was found that both antagonists led to cell membrane depolarization and promoted cell survival and LPS-activated TNFα after 24 h.

During their development in the BM, classical monocytes are imprinted with a transcriptional and epigenetic signature that facilitates their transition from the blood into tissues. It has been proposed however, that this signature is short lived, and that their release from controlling signals within the BM simultaneously triggers their differentiation into nonclassical monocytes, which are destined to remain within the vasculature. This generates only a short window of opportunity in which classical monocytes can extravasate into tissues to perform their diverse functions.[77] In human blood CD14$^+$ monocytes, we

made the striking observation that enhanced cell survival and LPS-triggered TNFα production after 24 h of differentiation are dependent on blockade of TRPM8 activity in the initial 3 h of culture. While the underlying mechanisms behind the susceptibility of CD14$^+$ monocytes to TRPM8 inhibition in this 3-h time frame remain uncharacterized, it is conceivable that this unique time frame represents the exhaustion of the short-lived transcriptional and epigenetic signature characteristic of classical monocytes. The concept of a sensitivity window within the lifespan of a monocyte in which the monocyte is highly susceptible to influence by environmental factors is reminiscent of the phenomenon of monocyte training that is elicited by various microbial challenges both in vivo and in vitro.[78,79] It will therefore be crucial to delineate the role of TRPM8 activity in this phenomenon in future studies. It should be noted however that phagocytic capacity in Mo-M was dependent on TRPM8 antagonism at later time points during the differentiation process, indicating some role for TRPM8 activity in CD14$^+$ monocytes after the first 3 h of culture, albeit with different downstream functional effects. Furthermore, membrane depolarization in response to AMTB is not exclusive to the cells in the early time window (data not shown), suggesting that TRPM8 activity does not simply cease after this point of differentiation.

Despite the identification of TRPM8 protein in human CD14$^+$ monocytes by both antibody staining and mass spectrometry, TRPM8 RNA was undetectable, an observation that we confirmed in our own as well as through the analysis of published RNA seq data in human primary monocytes,[59] which therefore excludes the possibility of expression of a TRPM8 isoform not detected by the qPCR primers we selected. It is possible that the disassociation between RNA and protein expression in CD14$^+$ monocytes reflects the relatively unstable and rapidly changing nature of classical monocytes. TRPM8 could be one of the genes affected upon release from the BM developmental niche, leading to rapid transcriptional repression but leaving some residual protein.

How TRPM8 activity contributes to the multiple and variable functional effects observed in human monocytes and their derivatives is an interesting area for further study. The close association between TRPM8 and PI(4,5)P$_2$ may be a critical angle to consider; in addition to being dependent on PI(4,5)P$_2$ for its activation, TRPM8 activity facilitates the hydrolysis of PI(4,5)P$_2$, via a Ca^{2+}-sensitive PLC isoform.[33] PI(4,5)P$_2$ in itself influences many signaling cascades and cellular processes, and notably is a substrate for other signal transducer enzymes such as PI3K that control cellular functions such as survival, proliferation, and migration.[80]

Our data demonstrate that the cation channel, TRPM8 is one of the signals that specifies the fate of human CD14$^+$ monocytes. Activity of this channel facilitates their transition to macrophages, which is importantly characterized by the acquisition of phagocytic properties and the down-regulation of proinflammatory responses to bacterial stimulation. Our data further highlight the importance of TRPM8 activity within the initial few hours of monocyte differentiation that is essential to control the early stages of their differentiation to macrophages. Understanding the underlying mechanisms that regulate TRPM8 activity in monocytes and exploring whether there are alterations to this

pathway in the context of disease and inflammation may allow for the identification of novel therapeutic targets.

AUTHORSHIP

Conceptualization: E. H., M. P., L. A. B., J. O. L., and A. J. S.; *methodology*: E. H., M. P., W. J. L., and R. B.; *formal analysis*: E. H., H. W. K., and R. B.; *investigation*: E. H., M. P., W. J. L., E. S. W., and R. B.; *writing- original draft*: E. H. and R. B. *Writing-Review & Editing*: H. W. K., M. P., J. O. L., and A. J. S.; *supervision*: J. O. L. and A. J. S.; *funding acquisition*: M. P., L. A. B., J. O. L., and A. J. S. *Equal contribution to the paper*: L.A.B. and J. O. L.

DISCLOSURE

J. O. L. has received honoraria for lecturing, consultancy, and advisory boards; an unrestricted grant for an investigator-led research project; and sponsorship to attend international conferences, from Takeda. A. J. S and L. A. B have received research funding from Takeda.

ORCID

Eve Hornsby https://orcid.org/0000-0002-2117-9164

Hamish W. King https://orcid.org/0000-0001-5972-8926

Madusha Peiris https://orcid.org/0000-0003-4429-5931

Wing-Yiu Jason Lee https://orcid.org/0000-0002-8524-3874

James O. Lindsay https://orcid.org/0000-0003-3353-9590

Andrew J. Stagg https://orcid.org/0000-0001-6588-0844

REFERENCES

1. Nahrendorf M, Swirski FK, Aikawa E, et al. The healing myocardium sequentially mobilizes two monocyte subsets with divergent and complementary functions. *J Exp Med*. 2007;204:3037-47. https://doi.org/10.1084/jem.20070885. Nov.

2. Trompette A, Gollwitzer ES, Pattaroni C, et al. Dietary fiber confers protection against Flu by shaping Ly6c. *Immunity*. 2018;48:992-1005.e8. https://doi.org/10.1016/j.immuni.2018.04.022. 05.

3. Moore KJ, Tabas I. Macrophages in the pathogenesis of atherosclerosis. *Cell*. 2011;145:341-55. https://doi.org/10.1016/j.cell.2011.04.005. Apr.

4. Krenkel O, Puengel T, Govaere O, et al. Therapeutic inhibition of inflammatory monocyte recruitment reduces steatohepatitis and liver fibrosis. *Hepatology*. 2018;67:1270-1283. https://doi.org/10.1002/hep.29544. 04.

5. Plantinga M, Guilliams M, Vanheerswynghels M, et al. Conventional and monocyte-derived CD11b(+) dendritic cells initiate and maintain T helper 2 cell-mediated immunity to house dust mite allergen. *Immunity*. 2013;38:322-35. https://doi.org/10.1016/j.immuni.2012.10.016. Feb.

6. Baillie JK, Arner E, Daub C, et al. Analysis of the human monocyte-derived macrophage transcriptome and response to lipopolysaccharide provides new insights into genetic aetiology of inflammatory bowel disease. *PLoS Genet*. 2017;13:e1006641. https://doi.org/10.1371/journal.pgen.1006641. 03.

7. Franklin RA, Liao W, Sarkar A, et al. The cellular and molecular origin of tumor-associated macrophages. *Science*. 2014;344:921-5. https://doi.org/10.1126/science.1252510. May.

8. Patel AA, Zhang Y, Fullerton JN, et al. The fate and lifespan of human monocyte subsets in steady state and systemic inflammation. *J Exp Med*. 2017;214:1913-1923. https://doi.org/10.1084/jem.20170355. Jul.

9. Bain CC, Bravo-Blas A, Scott CL, et al. Constant replenishment from circulating monocytes maintains the macrophage pool in the intestine of adult mice. *Nat Immunol*. 2014;15:929-937. https://doi.org/10.1038/ni.2967. Oct.

10. Jakubzick C, Gautier EL, Gibbings SL, et al. Minimal differentiation of classical monocytes as they survey steady-state tissues and transport antigen to lymph nodes. *Immunity*. 2013;39:599-610. https://doi.org/10.1016/j.immuni.2013.08.007. Sep.

11. Molawi K, Wolf Y, Kandalla PK, et al. Progressive replacement of embryo-derived cardiac macrophages with age. *J Exp Med*. 2014;211:2151-8. https://doi.org/10.1084/jem.20140639. Oct.

12. Shaw TN, Houston SA, Wemyss K, et al. Tissue-resident macrophages in the intestine are long lived and defined by Tim-4 and CD4 expression. *J Exp Med*. 2018;215:1507-1518. https://doi.org/10.1084/jem.20180019. Jun.

13. Tamoutounour S, Guilliams M, Montanana Sanchis F, et al. Origins and functional specialization of macrophages and of conventional and monocyte-derived dendritic cells in mouse skin. *Immunity*. 2013;39:925-38. https://doi.org/10.1016/j.immuni.2013.10.004. Nov.

14. Epelman S, Lavine KJ, Beaudin AE, et al. Embryonic and adult-derived resident cardiac macrophages are maintained through distinct mechanisms at steady state and during inflammation. *Immunity*. 2014;40:91-104. https://doi.org/10.1016/j.immuni.2013.11.019. Jan.

15. Schridde A, Bain CC, Mayer JU, et al. Tissue-specific differentiation of colonic macrophages requires TGFβ receptor-mediated signaling. *Mucosal Immunol*. 2017;10:1387-1399. https://doi.org/10.1038/mi.2016.142. 11.

16. Zigmond E, Bernshtein B, Friedlander G, et al. Macrophage-restricted interleukin-10 receptor deficiency, but not IL-10 deficiency, causes severe spontaneous colitis. *Immunity*. 2014;40:720-33. https://doi.org/10.1016/j.immuni.2014.03.012. May.

17. Schulthess J, Pandey S, Capitani M, et al. The short chain fatty acid butyrate imprints an antimicrobial program in macrophages. *Immunity*. 2019;50:432-445.e7. https://doi.org/10.1016/j.immuni.2018.12.018. Feb.

18. Goudot C, Coillard A, Villani AC, et al. Aryl hydrocarbon receptor controls monocyte differentiation into dendritic cells versus macrophages. *Immunity*. 2017;47:582-596.e6. https://doi.org/10.1016/j.immuni.2017.08.016. 09.

19. Gamrekelashvili J, Giagnorio R, Jussofie J, et al. Regulation of monocyte cell fate by blood vessels mediated by Notch signalling. *Nat Commun*. 2016;7:12597. https://doi.org/10.1038/ncomms12597. 08.

20. Yáñez A, Coetzee SG, Olsson A, et al. Granulocyte-monocyte progenitors and monocyte-dendritic cell progenitors independently produce functionally distinct monocytes. *Immunity*. 2017;47:890-902.e4. https://doi.org/10.1016/j.immuni.2017.10.021. 11.

21. Clapham DE. TRP channels as cellular sensors. *Nature*. 2003;426:517-24. https://doi.org/10.1038/nature02196. Dec.

22. Khalil M, Alliger K, Weidinger C, et al. Functional role of transient receptor potential channels in immune cells and epithelia. *Front Immunol*. 2018;9:174. https://doi.org/10.3389/fimmu.2018.00174.

23. Bertin S, Aoki-Nonaka Y, de Jong PR, et al. The ion channel TRPV1 regulates the activation and proinflammatory properties of CD4^{+} T cells. *Nat Immunol*. 2014;15:1055-1063. https://doi.org/10.1038/ni.3009. Nov.

24. Bertin S, Aoki-Nonaka Y, Lee J, et al. The TRPA1 ion channel is expressed in CD4+ T cells and restrains T-cell-mediated colitis

through inhibition of TRPV1. *Gut*. 2017;66:1584-1596. https://doi.org/10.1136/gutjnl-2015-310710. 09.

25. Krishnamoorthy M, Wasim L, Buhari FHM, et al. The channel-kinase TRPM7 regulates antigen gathering and internalization in B cells. *Sci Signal*. 2018;11. https://doi.org/10.1126/scisignal.aah6692. Jun.

26. Krishnamoorthy M, Buhari FHM, Zhao T, et al. The ion channel TRPM7 is required for B cell lymphopoiesis. *Sci Signal*. 2018;11. https://doi.org/10.1126/scisignal.aan2693. Jun.

27. Schappe MS, Szteyn K, Stremska ME, et al. Chanzyme TRPM7 mediates the Ca. *Immunity*. 2018;48:59-74.e5. https://doi.org/10.1016/j.immuni.2017.11.026. 01.

28. Di A, Gao XP, Qian F, et al. The redox-sensitive cation channel TRPM2 modulates phagocyte ROS production and inflammation. *Nat Immunol*. 2011;13:29-34. https://doi.org/10.1038/ni.2171. Nov.

29. Tseng HH, Vong CT, Kwan YW, Lee SM, Hoi MP. TRPM2 regulates TXNIP-mediated NLRP3 inflammasome activation via interaction with p47 phox under high glucose in human monocytic cells. *Sci Rep*. 2016;6:35016. https://doi.org/10.1038/srep35016. 10.

30. McKemy DD, Neuhausser WM, Julius D. Identification of a cold receptor reveals a general role for TRP channels in thermosensation. *Nature*. 2002;416:52-8. https://doi.org/10.1038/nature719. Mar.

31. Peier AM, Moqrich A, Hergarden AC, et al. A TRP channel that senses cold stimuli and menthol. *Cell*. 2002;108:705-15. Mar.

32. Tsavaler L, Shapero MH, Morkowski S, Laus R. Trp-p8, a novel prostate-specific gene, is up-regulated in prostate cancer and other malignancies and shares high homology with transient receptor potential calcium channel proteins. *Cancer Res*. 2001;61:3760-9. May.

33. Rohács T, Lopes CM, Michailidis I, Logothetis DE. PI(4,5)P2 regulates the activation and desensitization of TRPM8 channels through the TRP domain. *Nat Neurosci*. 2005;8:626-34. https://doi.org/10.1038/nn1451. May.

34. Liu L, Rohacs T. Regulation of the cold-sensing TRPM8 channels by phosphoinositides and G. *Channels (Austin)*. 2020;14:79-86. https://doi.org/10.1080/19336950.2020.1734266. Dec.

35. Vanden Abeele F, Zholos A, Bidaux G, et al. Ca2+-independent phospholipase A2-dependent gating of TRPM8 by lysophospholipids. *J Biol Chem*. 2006;281:40174-82. https://doi.org/10.1074/jbc.M605779200. Dec.

36. Andersson DA, Nash M, Bevan S. Modulation of the cold-activated channel TRPM8 by lysophospholipids and polyunsaturated fatty acids. *J Neurosci*. 2007;27:3347-55. https://doi.org/10.1523/JNEUROSCI.4846-06.2007. Mar.

37. Asuthkar S, Elustondo PA, Demirkhanyan L, et al. The TRPM8 protein is a testosterone receptor: i. Biochemical evidence for direct TRPM8-testosterone interactions. *J Biol Chem*. 2015;290:2659-69. https://doi.org/10.1074/jbc.M114.610824. Jan.

38. Asuthkar S, Demirkhanyan L, Sun X, et al. The TRPM8 protein is a testosterone receptor: iI. Functional evidence for an ionotropic effect of testosterone on TRPM8. *J Biol Chem*. 2015;290:2670-88. https://doi.org/10.1074/jbc.M114.610873. Jan.

39. Khajavi N, Reinach PS, Slavi N, et al. Thyronamine induces TRPM8 channel activation in human conjunctival epithelial cells. *Cell Signal*. 2015;27:315-25. https://doi.org/10.1016/j.cellsig.2014.11.015. Feb.

40. Genova T, Grolez GP, Camillo C, et al. TRPM8 inhibits endothelial cell migration via a non-channel function by trapping the small GTPase Rap1. *J Cell Biol*. 2017;216:2107-2130. https://doi.org/10.1083/jcb.201506024. 07.

41. Yang ZH, Wang XH, Wang HP, Hu LQ. Effects of TRPM8 on the proliferation and motility of prostate cancer PC-3 cells. *Asian J Androl*. 2009;11:157-65. https://doi.org/10.1038/aja.2009.1. Mar.

42. Sabnis AS, Reilly CA, Veranth JM, Yost GS. Increased transcription of cytokine genes in human lung epithelial cells through activation of a TRPM8 variant by cold temperatures. *Am J Physiol Lung Cell Mol Physiol*. 2008;295:L194-200. https://doi.org/10.1152/ajplung.00072.2008. Jul.

43. Jiang C, Zhai M, Yan D, et al. Dietary menthol-induced TRPM8 activation enhances WAT "browning" and ameliorates diet-induced obesity. *Oncotarget*. 2017;8:75114-75126. https://doi.org/10.18632/oncotarget.20540. Sep.

44. Wu SN, Wu PY, Tsai ML. Characterization of TRPM8-like channels activated by the cooling agent icilin in the macrophage cell line RAW 264.7. *J Membr Biol*. 2011;241:11-20. https://doi.org/10.1007/s00232-011-9358-6. May.

45. Khalil M, Babes A, Lakra R, et al. Transient receptor potential melastatin 8 ion channel in macrophages modulates colitis through a balance-shift in TNF-alpha and interleukin-10 production. *Mucosal Immunol*. 2016;9:1500-1513. https://doi.org/10.1038/mi.2016.16. 11.

46. Kume H, Tsukimoto M. TRPM8 channel inhibitor AMTB suppresses murine T-cell activation induced by T-cell receptor stimulation, concanavalin A, or external antigen re-stimulation. *Biochem Biophys Res Commun*. 2019;509:918-924. https://doi.org/10.1016/j.bbrc.2019.01.004. Feb.

47. de Jong PR, Takahashi N, Peiris M, et al. TRPM8 on mucosal sensory nerves regulates colitogenic responses by innate immune cells via CGRP. *Mucosal Immunol*. 2015;8:491-504. https://doi.org/10.1038/mi.2014.82. May.

48. Ramachandran R, Hyun E, Zhao L, et al. TRPM8 activation attenuates inflammatory responses in mouse models of colitis. *Proc Natl Acad Sci USA*. 2013;110:7476-81. https://doi.org/10.1073/pnas.1217431110. Apr.

49. Patro R, Duggal G, Love MI, Irizarry RA, Kingsford C. Salmon provides fast and bias-aware quantification of transcript expression. *Nat Methods*. 2017;14:417-419. https://doi.org/10.1038/nmeth.4197. Apr.

50. Soneson C, Love MI, Robinson MD. Differential analyses for RNA-seq: transcript-level estimates improve gene-level inferences. *F1000Res*. 2015;4:1521. https://doi.org/10.12688/f1000research.7563.2.

51. Love MI, Huber W, Anders S. Moderated estimation of fold change and dispersion for RNA-seq data with DESeq2. *Genome Biol*. 2014;15:550. https://doi.org/10.1186/s13059-014-0550-8.

52. Zhou Y, Zhou B, Pache L, et al. Metascape provides a biologist-oriented resource for the analysis of systems-level datasets. *Nat Commun*. 2019;10:1523. https://doi.org/10.1038/s41467-019-09234-6. 04.

53. Bligh EG, Dyer WJ. A rapid method of total lipid extraction and purification. *Can J Biochem Physiol*. 1959;37:911-7. https://doi.org/10.1139/o59-099. Aug.

54. Mirza SP, Halligan BD, Greene AS, Olivier M. Improved method for the analysis of membrane proteins by mass spectrometry. *Physiol Genomics*. 2007;30:89-94. https://doi.org/10.1152/physiolgenomics.00279.2006. Jun.

55. Geer LY, Markey SP, Kowalak JA, et al. Open mass spectrometry search algorithm. *J Proteome Res*. 2004;3:958-64. https://doi.org/10.1021/pr0499491. Sep-Oct.

56. Vaudel M, Barsnes H, Berven FS, Sickmann A, Martens L. SearchGUI: an open-source graphical user interface for simultaneous OMSSA and X!Tandem searches. *Proteomics*. 2011;11:996-9. https://doi.org/10.1002/pmic.201000595. Mar.

57. Vaudel M, Burkhart JM, Zahedi RP, et al. PeptideShaker enables reanalysis of MS-derived proteomics data sets. *Nat Biotechnol*. 2015;33:22-4. https://doi.org/10.1038/nbt.3109. Jan.

58. Valero M, Morenilla-Palao C, Belmonte C, Viana F. Pharmacological and functional properties of TRPM8 channels in prostate tumor cells. *Pflugers Arch*. 2011;461:99-114. https://doi.org/10.1007/s00424-010-0895-0. Jan.

59. Mirsafian H, Ripen AM, Leong WM, Manaharan T, Mohamad SB, Merican AF. Transcriptome landscape of human primary monocytes at different sequencing depth. *Genomics*. 2017;109:463-470. https://doi.org/10.1016/j.ygeno.2017.07.003. 10.

60. Tamoutounour S, Henri S, Lelouard H, et al. CD64 distinguishes macrophages from dendritic cells in the gut and reveals the

Th1-inducing role of mesenteric lymph node macrophages during colitis. *Eur J Immunol.* 2012;42:3150-66. https://doi.org/10.1002/eji.201242847. Dec.

61. Bouchot A, Millot JM, Charpentier S, et al. Membrane potential changes after infection of monocytes by Toxoplasma gondii. *Int J Parasitol.* 2001;31:1114-20. Aug.

62. Li C, Levin M, Kaplan DL. Bioelectric modulation of macrophage polarization. *Sci Rep.* 2016;6:21044. https://doi.org/10.1038/srep21044. Feb.

63. Lashinger ES, Steiginga MS, Hieble JP, et al. AMTB, a TRPM8 channel blocker: evidence in rats for activity in overactive bladder and painful bladder syndrome. *Am J Physiol Renal Physiol.* 2008;295:F803-10. https://doi.org/10.1152/ajprenal.90269.2008. Sep.

64. Almeida MC, Hew-Butler T, Soriano RN, et al. Pharmacological blockade of the cold receptor TRPM8 attenuates autonomic and behavioral cold defenses and decreases deep body temperature. *J Neurosci.* 2012;32:2086-99. https://doi.org/10.1523/JNEUROSCI.5606-11.2012. Feb.

65. Patel R, Gonçalves L, Leveridge M, et al. Anti-hyperalgesic effects of a novel TRPM8 agonist in neuropathic rats: a comparison with topical menthol. *Pain.* 2014;155:2097-107. https://doi.org/10.1016/j.pain.2014.07.022. Oct.

66. Bidaux G, Gordienko D, Shapovalov G, et al. 4TM-TRPM8 channels are new gatekeepers of the ER-mitochondria Ca. *Biochim Biophys Acta Mol Cell Res.* 2018;1865:981-994. https://doi.org/10.1016/j.bbamcr.2018.04.007. 07.

67. Wondergem R, Bartley JW. Menthol increases human glioblastoma intracellular Ca2+, BK channel activity and cell migration. *J Biomed Sci.* 2009;16:90. https://doi.org/10.1186/1423-0127-16-90. Sep.

68. Sundelacruz S, Levin M, Kaplan DL. Depolarization alters phenotype, maintains plasticity of predifferentiated mesenchymal stem cells. *Tissue Eng Part A.* 2013;19:1889-908. https://doi.org/10.1089/ten.tea.2012.0425.rev. Sep.

69. Smythies LE, Sellers M, Clements RH, et al. Human intestinal macrophages display profound inflammatory anergy despite avid phagocytic and bacteriocidal activity. *J Clin Invest.* 2005;115:66-75. https://doi.org/10.1172/JCI19229. Jan.

70. Bain CC, Scott CL, Uronen-Hansson H, et al. Resident and pro-inflammatory macrophages in the colon represent alternative context-dependent fates of the same Ly6Chi monocyte precursors. *Mucosal Immunol.* 2013;6:498-510. https://doi.org/10.1038/mi.2012.89. May.

71. Rivollier A, He J, Kole A, Valatas V, Kelsall BL. Inflammation switches the differentiation program of Ly6Chi monocytes from antiinflammatory macrophages to inflammatory dendritic cells in the colon. *J Exp Med.* 2012;209:139-55. https://doi.org/10.1084/jem.20101387. Jan 16.

72. Schilling T, Eder C. Non-selective cation channel activity is required for lysophosphatidylcholine-induced monocyte migration. *J Cell Physiol.* 2009;221:325-34. https://doi.org/10.1002/jcp.21857. Nov.

73. Yang J, Zhao Z, Gu M, Feng X, Xu H. Release and uptake mechanisms of vesicular Ca. *Protein Cell.* 2019;10:8-19. https://doi.org/10.1007/s13238-018-0523-x. 01.

74. Harrington AM, Hughes PA, Martin CM, et al. A novel role for TRPM8 in visceral afferent function. *Pain.* 2011;152:1459-68. https://doi.org/10.1016/j.pain.2011.01.027. Jul.

75. Klumpp D, Frank SC, Klumpp L, et al. TRPM8 is required for survival and radioresistance of glioblastoma cells. *Oncotarget.* 2017;8:95896-95913. https://doi.org/10.18632/oncotarget.21436. Nov.

76. Yapa KTDS, Deuis J, Peters AA, et al. Assessment of the TRPM8 inhibitor AMTB in breast cancer cells and its identification as an inhibitor of voltage gated sodium channels. *Life Sci.* 2018;198:128-135. https://doi.org/10.1016/j.lfs.2018.02.030. Apr.

77. Polletti S, Natoli G. Understanding spontaneous conversion: the case of the Ly6C. *Immunity.* 2017;46:764-766. https://doi.org/10.1016/j.immuni.2017.04.010. 05.

78. Quintin J, Saeed S, Martens JHA, et al. Candida albicans infection affords protection against reinfection via functional reprogramming of monocytes. *Cell Host Microbe.* 2012;12:223-32. https://doi.org/10.1016/j.chom.2012.06.006. Aug.

79. Netea MG, Joosten LA, Latz E, et al. Trained immunity: a program of innate immune memory in health and disease. *Science.* 2016;352:aaf1098. https://doi.org/10.1126/science.aaf1098. Apr.

80. Yu JS, Cui W. Proliferation, survival and metabolism: the role of PI3K/AKT/mTOR signalling in pluripotency and cell fate determination. *Development.* 2016;143:3050-60. https://doi.org/10.1242/dev.137075. 09.

SUPPORTING INFORMATION

Additional supporting information may be found in the online version of the article at the publisher's website.